Toxicology Reports 8 (2021) 1917–1929

Contents lists available at ScienceDirect

Toxicology Reports

journal homepage: www.elsevier.com/locate/toxrep

Co-exposure of sodium arsenite and uranyl acetate differentially alters gene expression in CD3/CD28 activated CD4+ T-cells

Jodi R. Schilz [a,*,1], Erica J. Dashner-Titus [b,1], Li Luo [c], Karen A. Simmons [b], Debra A. MacKenzie [b], Laurie G. Hudson [b]

[a] Division of Physical Therapy, School of Medicine, University of New Mexico, Albuquerque, NM, United States
[b] Department of Pharmaceutical Sciences, College of Pharmacy, University of New Mexico, Albuquerque, NM, United States
[c] Division of Epidemiology, Biostatistics and Preventive Medicine, Department of Internal Medicine, University of New Mexico, Albuquerque, NM, United States

ARTICLE INFO

Handling Editor: Dr. Aristidis Tsatsakis

Keywords:
Uranium
Arsenic
T-lymphocytes
Mixture toxicology

ABSTRACT

Communities in the western region of the United States experience environmental exposure to metal mixtures from living in proximity to numerous unremediated abandoned uranium mines. Metals including arsenic and uranium co-occur in and around these sites at levels higher than the United States Environmental Protection Agency maximum contaminant levels. To address the potential effect of these metals on the activation of CD4+ T-cells, we used RNA sequencing methods to determine the effect of exposure to sodium arsenite (1 μM and 10 μM), uranyl acetate (3 μM and 30 μM) or a mixture of sodium arsenite and uranyl acetate (1 μM sodium arsenite + 3 μM uranyl acetate). Sodium arsenite induced a dose dependent effect on activation associated gene expression; targeting immune response genes at the lower dose. Increases in oxidative stress gene expression were observed with both sodium arsenite doses. While uranyl acetate alone did not significantly alter activation associated gene expression, the mixture of uranyl acetate with sodium arsenite demonstrated a combined effect relative to sodium arsenite alone. The results demonstrate the need to investigate metal and metalloid mixtures at environmentally relevant concentrations to better understand the toxicological impact of these mixtures on T-cell activation, function and immune dysregulation.

1. Introduction

Abandoned uranium mines (AUMs) are scattered across the western region of the United States. Individuals living in close proximity to AUMs are at risk of exposure to heavy metal contaminants found in and around these sites. Uranium and arsenic frequently co-occur in water sources in the Western US and unregulated water sources close to AUMs show the two metals can co-occur at levels that each metal may exceed the highest level of a contaminant that is allowed in drinking water or the US EPA maximum contamination limit [1–5]. In the Southwest, a significant portion of the population relies on unregulated water sources, leaving these individuals vulnerable to arsenic and uranium exposures. Surface waters near the Jackpile uranium mine in Laguna Pueblo have measured uranium as high as 772 ug/L [6]. Populations living in close proximity to AUMs have higher levels of urinary metals, including uranium, compared to the general U.S. population supporting increased exposure based on location [7].

Health consequences such as increased risk of cancer, cardiovascular disease, inflammation and immune dysregulation have been associated with environmental exposure to metals such as arsenic and uranium [8–11]. Studies have shown that populations living near AUMs have an increased likelihood of developing multiple chronic diseases [12–15]. Additionally, uranium consumption through drinking water is associated with increased detection of autoantibodies to native DNA and/or chromatin [16]. A variety of studies, including *in vitro*, animal and population studies, reveal that exposure to metals may induce immune dysregulation through altered expression of key immune regulators, oxidative stress, induced apoptosis, and impaired lymphocyte activation

Abbreviations: APC, antigen presenting cell; AUM, abandoned uranium mine; DEG, differentially expressed gene; GCLM, glutamate-cysteine ligase; HMOX1, heme oxygenase 1; IFNγ, interferon gamma; IL-2, interleukin 2; MHC, major histone compatibility complex; NQO1, NAD(P)H quinone dehydrogenase; PCA, principal component analysis; SOD1, super oxide dismutase 1; TCR, T-cell receptor; Th, T-helper.

* Corresponding author.
E-mail address: jschilz@salud.unm.edu (J.R. Schilz).
[1] These authors contributed equally to the work.

https://doi.org/10.1016/j.toxrep.2021.11.019
Received 4 June 2021; Received in revised form 19 October 2021; Accepted 25 November 2021
Available online 27 November 2021

and function [17–21]. Arsenic is able to modify cytokine production in response to T-cell activation [22,23] possibly altering the ratio of T-cell populations [24,25]. Less is known about uranium and effects on immune function. However, people with a high lifetime exposure to uranium were shown to have decreased white blood cell and lymphocyte counts and increased eosinophil counts indicating immune dysregulation [19]. Decreased natural killer and T-lymphocyte absolute counts were seen in people living near a uranium mine and displaying high uranium blood levels [26]. Additionally in vitro and in vivo studies demonstrate altered expression of cytokines in response to uranium exposure which may lead to changes in T-cell ratios [18,20].

Naïve T-cells are produced by the thymus and, after release, are activated in secondary lymphoid tissues when they encounter antigen-presenting cells. Complete activation of naïve T-cells requires binding of the T-cell receptor (TCR) to the major histocompatibility complex (MHC) on an antigen presenting cell as well as costimulation though CD28. Combined TCR activation and costimulation through CD28 initiates downstream signaling cascades that reinforce proliferation signals and prepare the cell for both production of, and response to, cytokines that will determine the T-cell lineage. Alterations to activation including the strength and weakness of TCR and CD28 signaling or a lack of costimulation has been associated with alterations in Th1 and Th2 differentiation and hyporesponsiveness [27].

Studies support that arsenic disrupts T-cell activation [22,23,25,28]. However, most in vitro studies investigating arsenic-induced changes in gene expression during T-cell activation examine a limited number of genes through RT-PCR or microRNA panels [25,29,30] often in mixed T-cell populations (CD3+) [25,29]. This study is unique because it investigates overall gene expression changes in CD4+ T-cells due to sodium arsenite and uranyl acetate.

The alteration of T-cell activation by metals such as arsenic and uranium may play a role in the immune dysfunction found in populations living near AUMs. Therefore, it is crucial to understand the effect of these metals on human T-lymphocytes. In this toxicological study we test the effects of sodium arsenite and uranyl acetate alone or in combination on transcriptional changes induced following T-cell activation in normal human CD4+ T-cells. Despite population evidence suggesting that exposure to uranium can target immune cells; there are few T-cell specific studies and no studies investigating the combination of sodium arsenite and uranyl acetate on activation of CD4+ T-cells. In this study we find dose-dependent sodium arsenite effects on T-cell activation and combined impacts in the presence of both sodium arsenite plus uranyl acetate that are not seen with either metal alone.

2. Materials and methods

2.1. Chemicals

Uranium, as uranyl acetate (in the form of $UO_2(CH_3OCO)_2$ $2H_2O$) (99.6 % purity) comprised of 99.9 % ^{238}U and 0.1 % ^{235}U according to the product's technical bulletin, was purchased from Electron Microscopy Science (Hatfield, Pennsylvania). Uranyl acetate had a radioactive activity of 0.51 μCi g^{-1} and was handled according to the regulations set forth by the Radiation Safety office at the University of New Mexico. Arsenic, as sodium arsenite (in the form of $AsNaO_2$) (99 % purity) from Sigma-Aldrich (St. Louis, Missouri) was used for experimental treatments. Ten millimolar stock solutions of uranyl acetate and one hundred millimolar stock solutions of sodium arsenite were prepared in MilliQ water and sterilized using a 0.22-μm syringe filter. Working solutions were prepared by diluting the stock with complete cell growth medium.

2.2. Cell culture

Human CD4+ T-cells were purchased from Stemcell Technologies (Cambridge, Massachusetts). Cells were isolated from a 25-year-old male, nonsmoker (Catalog#70026, Lot 1709150078 and Donor #D001004147). Cells were thawed according to manufacturer's recommendation and resuspended at a concentration of 1×10^6 cells/mL in ImmunoCult™-XF T-Cell Expansion Medium from Stemcell Technologies. In an effort to model alterations in T-cell receptor activation in a chronically exposed population, cells were first maintained for 24 h in a humidified incubator with 5% CO_2 with metal (10 μM sodium arsenite (1299.1 μg/L NaAs or 749.2 μg/L As), 1 μM sodium arsenite (129.91 μg/L NaAs or 74.92 μg/L As), 3 μM uranyl acetate (1272.4 μg/L UA or 713.81 μg/L U), 30 μM uranyl acetate (12,724 μg/L UA or 7138.16 μg/L U) and 1 μM sodium arsenite + 3 μM uranyl acetate) or without metal. The cells were then activated with a soluble tetrameric (mouse/rat) antibody CD3/CD28 T-cell activator from Stemcell Technologies (catalog #10971) at a concentration of 25 μL/mL and allowed to continue to incubate with metal (experimental conditions listed above) or without metal (activated control) for an additional 48 h. The experimental conditions were independently repeated three times using CD4+ T-cells from the same donor. In addition to the CD4+ T-cells (25-year-old male, nonsmoker) purchased from Stemcell for the original RNA sequencing experiment, cells from another 27-year-old male (Catalog# 70500, Lot: Bx35025, Donor #RV01000282), nonsmoker and a 36-year-old female (Catalog# 70500.1, Lot: 1000029100, Donor #CE0006038), nonsmoker were isolated using the EasySep™ Human Naïve CD4+ T cell isolation kit II (Catalog #17555) from leukopaks purchased from StemCell technologies (Cambridge, Massachusetts). All cells used were determined to be >90 % CD4+. Cells isolated from leukopaks were treated with the described metals and activated for PCR validation of RNA sequencing results. Overall viability after metal treatment and activation was assessed using Trypan blue dye after 72 h (24 h metal pretreatment +48 h activation in the presence or absence of metal) for each PCR validation donor used in this study. The average donor cell death is reported as follows: activated control (16 %), 1 μM sodium arsenite (21 %), 10 μM sodium arsenite (27 %), 3 μM uranyl acetate (18 %) and 30 μM uranyl acetate (18 %) treatment (Supplemental Fig. 1).

2.3. RNA isolation

Cells were washed one time in room temperature 1X DPBS from Sigma Life Science (St. Louis, Missouri) and resuspended in buffer RLT provided in an RNeasy Mini Kit from Qiagen (Valencia, California). The cell lysate was homogenized using the QIAshredder from Qiagen and RNA was isolated using the RNeasy Mini Kit according to the manufacturers' protocols.

The nucleic acid purity was conducted by measuring the UV absorbance using a NanoDrop ND 1000 UV–vis Spectrophotometer from Thermo Fisher Scientific (Waltham, Massachusetts) to determine the concentration, 260/280, and 260/230 ratios. RNA concentration was determined using the RNA Assay kit on the Qubit 2.0 fluorometer from Invitrogen (Carlsbad, California). The integrity and quality of total RNA was evaluated by using the 2100 Bioanalyzer from Agilent (Santa Clara, California) with the Agilent RNA 6000 Nano Kit. Only RNA samples with a minimum RIN value $\geq$ 8.0 were used for further analysis.

2.4. RNA sequencing methods

Single-end sequencing, 75 base pairs read length was performed on all samples by the Illumina Next-Seq 500 platform by the National Center for Genome Resources (Santa Fe, New Mexico). Gene expression for all samples were computed as a measure of the total number of reads from individual samples uniquely aligning to the GRCh38.p12 version of the human reference genome (Genome FASTA file) and further binned by genic coordinates using the information provided in the annotation file (Genome annotation in GFF3 file).

2.5. Processing of RNA sequencing data

Due to the sample size and exploratory nature of the study, low count gene filtering was performed to ensure sequencing data quality while not being overly aggressive when excluding genes. We retained genes that had at least 5 read counts in at least one of the samples for further analysis. Differential expression analysis was conducted for the pre-filtered genes using R/Bioconductor package DESEQ2 [31,32]. Expression level was assessed as the gene counts divided by sample-specific size factors, and performed normalization using the algorithm implemented in the DESEQ2 package. The sample size factor was calculated by the median of the ratios of gene counts to the geometric mean across samples as the reference. The reference transcriptome used to determine DEGs for the activated control cells is the unactivated cells whereas the reference transcriptome used to determine DEGs due to metal treatment + activation are the activated cells without metal treatment. The RNA sequencing data is available for download from the EDI repository using study accession number: doi:10.6073/pasta/d1f37c312b10bc225f600cbea28788dc [33].

2.6. Functional enrichment analysis

To further explore the functions and biological pathways that might be altered by metal treatment, DEGs identified between unactivated CD4+ T-cells and CD4+ T-cells activated with CD3/CD28 for 48 h, and CD4+ T-cells pre-treated with metal for 24 h and then activated with CD3/CD28 for 48 additional hours compared to activation alone were input into Cytoscape v3.7.1 plug-in software, ClueGO v2.5.4 [34] for biological process enrichment analysis using Gene Ontology (GO, http://www.geneontology.org/) and Reactome pathway enrichment (https://reactome.org/content/detail/R-HSA-163809) [35,36]. Biological process and Reactome pathway enrichment analysis was performed with Cytoscape v3.7.1 plug-in software, ClueGO v2.5.4 [34], two-sided hypergeometric test to calculate the importance of each term was selected and Bonferroni step-down, and Kappa score level of 0.4 were used for P value correction. The adjusted *p*-value after Bonferroni correction was set at 0.05. The percentage for overlapping terms to be merged into another group was set at 50 %. The group leading term is the most significant term from a group and subterms are defined as terms with a lower *p*-value that were still significantly enriched.

2.7. PCR validation

In addition to the CD4+ T-cells isolated from the original 25-year-old male, nonsmoker, CD4+ T-cells from another 27-year-old male, nonsmoker and a 36-year-old female, nonsmoker were isolated, treated with the described metals and activated for PCR validation of RNA sequencing results. Quantitative real-time PCR (RT-qPCR) was used to examine a subset of relevant genes including both differentially expressed genes and genes unchanged by activation and metal treatment. The High Capacity cDNA Reverse Transcription Kit from Thermo Fisher Scientific was used to synthesize cDNA from 1 μg of RNA. SYBR Green PCR primers acquired from Bio-Rad (Hercules, California) are listed in Table 1. RT-qPCR was performed in triplicate using iTaq Universal SYBR Green Supermix from Bio-Rad on the BioRad CFX384 PCR System. The following cycling parameters were used: initial denaturation at 95 °C for 30 s, then 40 amplification cycles consisting of a 5 s denaturation step at 95 °C and a 30 s annealing/elongation step at 60 °C.Gene expression changes were calculated using the double delta Ct analysis method with 18S as a housekeeping gene.

Table 1
PCR primer list.

Gene	Forward sequence (5′ → 3′)	Reverse sequence (5′ → 3′)
18S	CGGAGGTTCGAAGACGATCAGATA	TTGGTTTCCCGGAAGCTGCC
IFNG	GGTTCTCTTGGCTGTTACT	CCATTATCCGCTACATCTGA
HMOX1	TCCTGGCTCAGCCTCAAATG	CGTTAAACACCTCCCTCCCC
NQO1	CGCAGACCTTGTGATATTCCAG	CGTTTCTTCCATCCTTCCAGG
IL2	BioRad proprietary qHsaCID0015409	
FZD4	BioRad proprietary qHsaCID0014233	
CTLA4	BioRad proprietary qHsaCED0003794	
CMPK2	BioRad proprietary qHsaCID0015030	
OAS3	BioRad proprietary qHsaCID0012667	

2.8. Statistical methods

Read counts for the RNA sequencing samples were normalized to account for differences in sequencing depth and library sizes using methods implemented within the DESEQ2 package. Negative binomial generalized linear model was fitted for each gene to assess the difference in gene expression. Fold changes were calculated to estimate the magnitude of effect sizes, and p values were calculated using the Wald tests to examine statistical significance. Multiple comparisons were controlled for using the Benjamini–Hochberg false discovery rate (FDR) method. Statistical significance was considered at the FDR adjusted p-value <0.10 due to the exploratory nature of this study where the sample sizes and effect sizes are limited. We conducted Principal Component Analysis (PCA) to explore the clustering of samples with similar expression patterns. All RNA sequencing statistical tests were two-sided and analyzed using R 3.6.1 (http:// www.R-project.org/). Consistencies between the RNA sequencing and PCR validation results in Donor 1 were tested using a Spearman's correlation. Comparisons between the PCR delta-CT of the unactivated CD4+ T-cells compared to the activated control for each donor were calculated using a *T*-test. Comparisons between the PCR delta-CT of the treatment groups and their activated control for each donor were calculated using a two way ANOVA with a Dunnett's post hoc comparison.

3. Results

3.1. Gene expression changes upon T-cell activation

Global gene expression changes were compared between unactivated

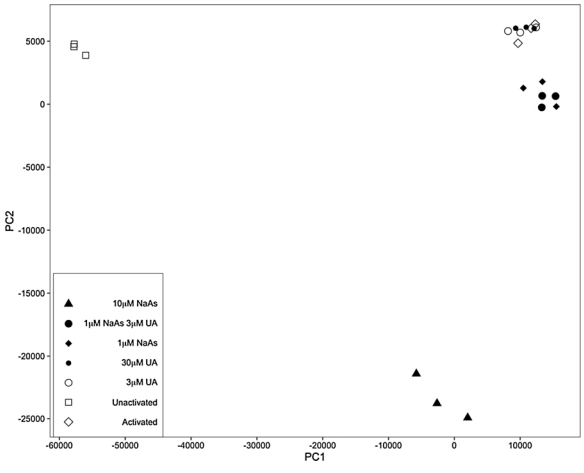

Fig. 1. Principal component analysis of differentially expressed genes. Each symbol represents an individual experiment while each shape indicates the treatment group. In the principal component analysis, the first component (PC1) separates samples based on activation and explains 78.5 % of the variance and the second component (PC2) separates samples based on metal treatment and explains 13.2 % of the variance. Unactivated – unactivated CD4+ T-cells, Activated – CD4+ T-cells activated with CD3/CD28 for 48 h, all other samples were pre-treated with the indicated metal concentration for 24 h before activation with CD3/CD28 for an additional 48 h. Three independent experiments per treatment group are shown. NaAs – sodium arsenite, UA – uranyl acetate.

CD4 + T-cells and T-cells activated with CD3/CD28 for 48 h. As shown in Fig. 1 (PC1 vs PC2) there is separation between the unactivated CD4+T-cells and all activated samples based on the first principle component. The activated CD4+ T-cells showed significant expression changes in a total of 12,889 genes compared to the unactivated CD4+ T-cell control; 6017 genes were significantly upregulated and 6872 genes were significantly downregulated. To verify activation, gene expression changes between unactivated CD4+ T-cells and CD4+ T-cells activated with CD3/CD28 were compared for a select set of early activation and post co-stimulation genes (Table 2). For example, activation and co-stimulation markers including C-Type Lectin Domain Family 2, Member C (*CD69),* interleukin 2 receptor subunit alpha *(IL2RA),* interferon gamma *(IFNG),* tumor necrosis factor alpha *(TNFA),* interleukin 2 *(IL2),* lymphocyte activating 3 *(LAG3),* cytotoxic T-lymphocyte associated protein 4 *(CTLA4)*, and inducible T-cell costimulatory (*ICOS)* have been reported in the literature to increase with activation and were upregulated in this study (Table 2) [25,37–39]. The results confirm that activated T-cell associated gene expression changes occurred and will be used as a baseline to compare the effects of metal treatment on activation.

3.2. Sodium arsenite alters gene expression changes detected upon T-cell activation

The potential perturbation of T-cell activation by sodium arsenite was tested by pretreating unactivated CD4+ T-cells with 10 μM (high dose) or 1 μM (low dose) sodium arsenite for 24 h and then adding a soluble CD3/CD28 antibody to induce activation. In order to assess dose dependent gene expression changes the 10 μM (high dose) sodium arsenite was chosen because it is more toxic and was expected to induce a response whereas the 1 μM (low dose) sodium arsenite better represents environmental levels. The metal concentration was readjusted and activation continued for an additional 48 h in the presence of sodium arsenite. RNA-sequencing analysis was performed on the initial donor and PCR validation was performed on all 3 donors.

RNA-sequencing analysis revealed a dose dependent perturbation of T-cell activation associated gene expression with sodium arsenite treatment. The second principle component separates samples based on metal treatment and explains 13.2 % of the variance in gene expression between the metal treatment groups. The second principle component in the PCA plot illustrates that samples activated in the presence of 10 μM sodium arsenite varied greatly from T-cells activated without metal (activation alone) and T-cells activated in the presence of the other metal treatments including the lower sodium arsenite dose (Fig. 1).

Activation in the presence of 10 μM sodium arsenite significantly altered the expression of 6795 genes compared to activation alone; 3269 genes were upregulated and 3526 were down regulated (Supplemental Table 1). Activation in the presence of 10 μM sodium arsenite decreased the expression of 6 and increased the expression of 3 of the activation and costimulation markers compared to activation alone (Table 2). Key markers of T-cell subtype identification were evaluated to determine the effect of sodium arsenite on differentiation in the absence of added stimulation factors. High dose sodium arsenite appears to alter markers of differentiation in major T-cell subtypes (Table 2), which has been observed in sodium arsenite exposed populations [40,41].

CD3/CD28 activation increased the expression of the oxidative stress genes heme oxygenase 1 (*HMOX1)*, *NAD(P)H quinone dehydrogenase (NQO1)*, *super oxide dismutase 1 (SOD1)* and glutamate-cysteine ligase (*GCLM)* but decreased expression of NADPH oxidase activator 1 (*NOXA1)* (Table 3). High dose sodium arsenite treatment (10 μM) significantly increased expression of all of these genes above activation alone (Table 3). The stress response gene *HMOX1* was the top differentially expressed gene when T-cells were activated in the presence of 10 μM sodium arsenite and along with upregulation of *NOXA1*, *SOD1* and *NQO1* indicates sodium arsenite-induced upregulation in oxidative stress at this concentration.

Low dose (1 μM) sodium arsenite had a more modest effect on T-cell activation associated gene expression. As shown in Fig. 1, the second principle component shows that samples activated in the presence of 1 μM sodium arsenite differed from activation alone, but to a lesser degree than T-cells activated in the presence of 10 μM sodium arsenite, thereby indicating dose dependence for the sodium arsenite effect. Activation in

Table 2
Log 2 fold-change of metal-induced alterations in genes influenced by T-cell receptor activation.

			Relative to Activated				
Gene Name	Ensembl ID	Activated	1 μM NaAs	10 μM NaAs	3 μM UA	30 μM UA	1 μM NaAs + 3 μM UA
Activation/costimulation markers							
IL2	ENSG00000109471.5	**5.65**[a]	−0.28	1.29	0.09	0.12	0.14
CD69	ENSG00000110848.8	**3.12**[a]	0.21	**0.35**[b]	0.16	0.08	0.11
TNFA	ENSG00000228978.2	**3.4**[a]	−0.01	**0.27**[b]	0.03	0.14	0.01
IL2RA (CD25α)	ENSG00000134460.18	**6.14**[a]	0.09	**−0.81**[b]	0.01	0.03	0.04
IL2RB (CD25β)	ENSG00000100385.14	**3.69**[a]	−0.11	**−1.50**[b]	−0.08	−0.08	−0.14
ICOS	ENSG00000163600.13	**5.40**[a]	−0.11	**−1.27**[b]	−0.08	−0.09	−0.16
CTLA4	ENSG00000163599.17	**10.54**[a]	−0.16	**−3.12**[b]	−0.01	0.01	−0.18
LAG3 (CD223)	ENSG00000089692.9	**2.11**[a]	**−0.45**[b]	**−3.14**[b]	0.07	−0.03	**−0.44**[b]
IFNG	ENSG00000111537.5	**5.90**[a]	**−0.58**[b]	**−3.58**[b]	−0.10	−0.02	**−0.40**[b]
Th1 markers							
IL27	ENSG00000197272.2	**2.75**[a]	−1.60	**−3.35**[b]	−0.69	−1.00	−0.59
STAT1	ENSG00000115415.20	**1.70**[a]	−0.19	**1.05**[b]	0.05	−0.09	−0.21
TBX21	ENSG00000073861.3	**3.04**[a]	−0.49	**−0.6**[b]	−0.08	−0.08	−0.37
Th2 markers							
IL4	ENSG00000113520.11	**4.92**[a]	0.37	0.27	0.00	−0.05	0.56
GATA3	ENSG00000107485.18	**0.41**[a]	0.04	−0.14	−0.04	−0.03	−0.01
IL6	ENSG00000136244.12	**6.34**[a]	−0.09	0.47	−0.20	0.09	0.15
Th17 markers							
IL21	ENSG00000138684.9	**7.92**[a]	−0.98	**−2.08**[b]	0.07	−0.10	−1.07
RORC	ENSG00000143365.19	**−0.87**[a]	−0.68	**−2.27**[b]	0.04	0.07	**−1.02**[b]
IL17A	ENSG00000112115.7	**8.21**[a]	**−0.60**[a]	**−4.07**[b]	−0.18	0.19	−0.43
Treg markers							
TGFB1	ENSG00000105329.10	**0.27**[a]	−0.01	**−0.38**[b]	−0.01	0.02	−0.08
FoxP3	ENSG00000049768.16	**2.43**[a]	0.04	−0.29	0.00	−0.12	0.06

Abbreviations: NaAs, sodium arsenite; UA, uranyl acetate. Results based on RNA obtained from donor 1.
[a] P-value ≤ 0.1 using Wald tests to compare activation vs unactivated.
[b] P-value ≤ 0.1 using Wald tests to compare metal treated groups vs. activated.

Table 3
Log 2 fold-changes of select oxidative stress responsive genes.

			Relative to Activated				
Gene Name	Ensembl ID	Activated	1 μM NaAs	10 μM NaAs	3 μM UA	30 μM UA	1 μM NaAs + 3 μM UA
HMOX1	ENSG00000100292.17	**1.33**[a]	**4.61**[b]	**8.79**[b]	0.12	0.25	**4.67**[b]
NQO1	ENSG00000181019.13	**2.17**[a]	**0.77**[b]	**1.87**[b]	0.02	0.00	**0.77**[b]
NOXA1	ENSG00000188747.8	**−2.38**[a]	0.25	**1.36**[b]	−0.43	−0.09	−0.20
GCLM	ENSG00000023909.10	**0.59**[a]	**0.66**[b]	**1.26**[b]	0.01	0.01	**0.67**[b]
SOD1	ENSG00000142168.15	**0.57**[a]	0.25	**0.77**[b]	0.00	0.04	**0.31**[b]

Abbreviations: As, sodium arsenite; U, uranyl acetate Results based on RNA obtained from donor 1.
[a] P-value ≤ 0.1 using Wald tests to compare activation vs unactivated.
[b] P-value ≤ 0.1 using Wald tests to compare metal treated groups vs. activated.

the presence of 1 μM sodium arsenite showed significant changes in expression of 142 genes compared to activation alone, 104 were downregulated and 38 were upregulated (Supplemental Table 2). Comparing the DEGs between the 10 μM and 1 μM sodium arsenite treatments there were 121 genes that were significantly changed with both the high and low dose sodium arsenite treatment (Fig. 2). Eighty-three were downregulated and 38 were upregulated. Twenty-one genes were significantly changed in the 1 μM sodium arsenite group treatment alone, 19 were downregulated and 2 were upregulated. The 21 genes significant in the 1 μM sodium arsenite treatment group had a larger effect size (larger magnitude of log fold changes relative to the activated samples) compared to the higher dose 10 μM sodium arsenite treatment. Meanwhile the majority of these genes showed smaller variation in the 1 μM sodium arsenite group compared to the 10 μM sodium arsenite group, resulting in statistically significant results. Eleven of the 21 genes significant in the 1 μM sodium arsenite treatment group were enriched in an immune related biological process (Supplemental Table 6). Expression changes with 1 μM sodium arsenite treatment were significant in 3 of the markers of T-cell activation/costimulation and similar trends between the 1 μM sodium arsenite and 10 μM treatments were observed in the key markers of T-cell subtype identification with the highest effects in genes associated with Th1 and Th17 cell subtypes (Table 2). Sodium arsenite at the environmentally relevant dose of 1 μM increased the oxidative stress markers *HMOX1*, *NQO1* and *GCLM* compared to activation alone (Table 3), indicating an oxidative stress response is sustained at the lower dose.

3.3. Uranyl acetate does not alter gene expression changes detected upon T-cell activation

Gene expression analysis revealed that neither 3 μM nor 30 μM uranyl acetate treatment significantly altered any of the 18,381 genes compared to activation alone. The second principle component in the PCA plot illustrates that samples activated in the presence of 3 or 30 μM uranyl acetate did not vary from activation alone (Fig. 1). There were no significant changes in selected T-cell activation/costimulation markers, markers of T-cell subtype identification (Table 2) or oxidative stress markers (Table 3). Previous inductively coupled mass spectrometry experiments have confirmed that uranyl acetate can enter and accumulate in an immortalized T-cell line (Jurkats) at both the 3 μM and 30 μM doses indicating it is likely entering the T-cell but not altering gene expression [42].

3.4. Gene expression changes upon T-cell activation in the presence of a metal mixture

While uranyl acetate treatment alone did not alter gene expression induced by T-cell activation, we investigated whether the mixture of uranyl acetate and sodium arsenite present during activation influenced gene expression profiles compared to sodium arsenite alone. T-cell activation in the presence of a mixture of 1 μM sodium arsenite and 3 μM uranyl acetate significantly altered the expression of 191 genes; 156 genes were downregulated and 35 were upregulated (Supplemental Table 3). DEGs identified with the 1 μM sodium arsenite treatment (compared to activation alone) and 1 μM sodium arsenite + 3 μM uranyl

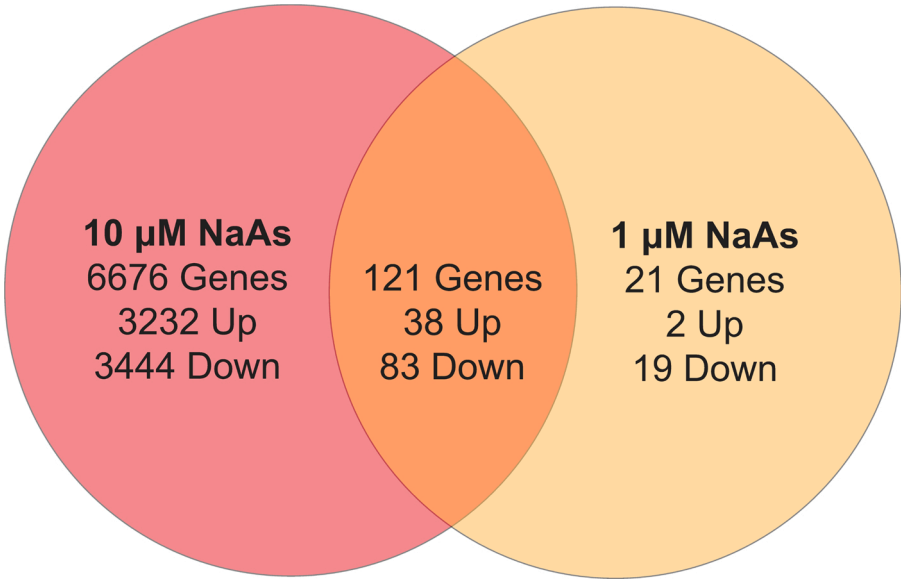

Fig. 2. Comparison of DEGs between 10 μM and 1 μM sodium arsenite (NaAs) treatments. Venn diagram comparing the differential expression of cells treated with 10 μM sodium arsenite (NaAs) and 1 μM sodium arsenite (NaAs) compared to activation.

acetate treatment (compared to activation alone) were analyzed (Fig. 3). Forty genes altered with the 1 μM sodium arsenite treatment were unchanged by the addition of uranyl acetate. One hundred and two genes were altered by both the 1 μM sodium arsenite and 1 μM sodium arsenite + 3 μM uranyl acetate treatments. Eighty-nine genes were significantly altered by only the mixture (bolded in Supplemental Table 3). These 89 genes had a larger effect size resulting in statistical significance. Results indicate that the low dose uranyl acetate modifies gene expression when combined with low dose sodium arsenite, indicating a potential mixed-metal effect.

3.5. Pathway analysis

DEGs due to activation in the presence of 10 μM sodium arsenite compared to activation alone were uploaded into ClueGO v.2.5.0 with a Cytoscape v.3.7.1 plugin [34] to detect biological process and Reactome pathways that were significantly enriched. The leading enriched biological process terms with ≥40 % associated genes are listed in Table 4. Sub-terms with a lower adjusted *p*-value that were organized under a leading biological process term and were associated with T-cell activation and/or immune response are listed in italics under the leading biological process term. There were 56 leading enriched biological process terms (highest p value and % genes per term) identified (Supplemental Table 4). Significantly enriched terms associated with T-cell activation include: "positive regulation of INFɣ production, IL-1 mediated signaling pathway (T-cell receptor signaling and innate immune response), regulation of cytokines, myeloid cell homeostasis (immune system development, regulation of T- cell activation/differentiation), and positive regulation of DNA-binding transcription factor activity (NfKB activity)". Results indicate that the presence of sodium arsenite during activation alters pathways associated with T-cell activation and function. As shown in Table 4 and Supplemental Table 4, the high dose sodium arsenite treatment also leads to expression changes in genes associated with a variety of cellular processes not necessarily related to immune function.

The leading enriched Reactome pathway terms with ≥40 % associated genes are listed in Table 5. There were 24 leading enriched pathway terms (highest p value and % genes per term) identified and sub-terms are listed in italics under the leading pathway term (Supplemental Table 5). The majority of the pathways associated with T-cell activation were organized under the leading term "ER-phagosome pathway" including "antigen processing-cross presentation, cytokine signaling in immune system, signaling by interleukins and adaptive/innate immune system" (Table 5). Non-T-cell specific pathways included "Apoptosis, G0 and early G1, metabolism of proteins, downstream signal transduction

Table 4
Biological process enrichment terms with >40 % genes for 10 μM sodium arsenite treatment.

Go Term	Term p-value	% Genes
Regulation of transcription involved in G1/S transition of mitotic cell cycle	1.24E-06	67.57
Response to amino acid starvation	1.19E-06	59.02
Negative regulation of sister chromatid segregation	4.88E-07	57.75
Cell cycle DNA replication	9.95E-08	56.18
Positive regulation of interferon-gamma production:	1.83E-06	55.13
[a]*T-helper 1 type immune response, regulation of adaptive immune response based on somatic recombination of immune receptors*		
Interleukin-1-mediated signaling pathway:	9.11E-08	52.07
[a]*Innate immune response-activating signal transduction, T cell receptor signaling pathway*		
Cytoskeleton-dependent cytokinesis	2.13E-07	50.38
Regulation of type I interferon production	3.50E-08	50.00
Regulation of cytokinesis	2.28E-05	47.46
Negative regulation of cell cycle process	1.41E-17	46.79
Cyclin-dependent protein kinase activity	2.84E-06	45.66
Myeloid cell homeostasis:	7.79E-07	45.45
[a]*Immune system development, regulation of T cell activation, regulation of T cell differentiation*		
Positive regulation of cell cycle	4.87E-16	45.12
Regulation of cell cycle process	3.82E-30	45.00
Sterol metabolic process	1.82E-06	44.04
Microtubule cytoskeleton organization	2.60E-13	41.86
Positive regulation of cytokine production	4.40E-10	40.67
Positive regulation of DNA-binding transcription factor activity:	2.21E-06	40.50
[a]*Positive regulation of NfKB transcription factor activity*		
Protein autophosphorylation	5.42E-06	40.48
Protein modification by small protein removal	1.47E-06	40.48
DNA conformation change	3.26E-06	40.16
Response to hypoxia	1.73E-07	40.13
In utero embryonic development	3.29E-07	40.00

[a] Subterms relevant to immune parameters in italics.

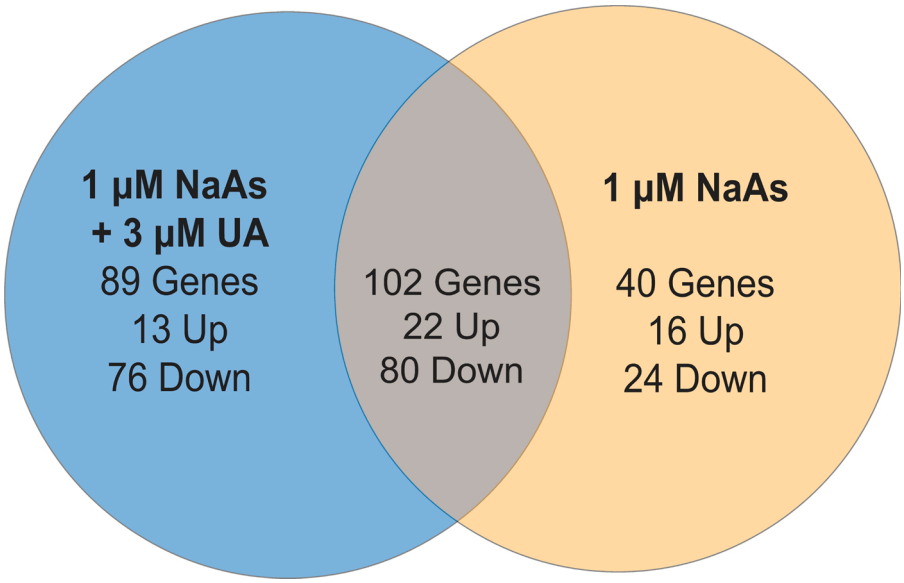

Fig. 3. Comparison of DEGs from 1 μM sodium arsenite + 3 μM uranyl acetate and 1 μM sodium arsenite treatments. Venn diagram comparing the differential expression of cells treated with 1 μM sodium arsenite (NaAs) + 3 μM uranyl acetate (UA) and 1 μM sodium arsenite (NaAs) treatments compared to activation.

Table 5
Reactome pathway enrichment terms with >40 % genes for 10 μM sodium arsenite treatment.

Go Term	Term p-value	% Genes
Polo-like kinase mediated events	1.86E-04	93.75
Condensation of Prometaphase Chromosomes	3.46E-02	90.91
Translesion synthesis by REV1	2.80E-02	81.25
Cholesterol biosynthesis	4.53E-04	80.00
G0 and Early G1	3.51E-03	74.07
TP53 Regulates Transcription of Cell Cycle Genes	3.78E-05	69.39
Downstream signal transduction	2.50E-02	68.97
Transcriptional Regulation by E2F6	4.49E-03	68.57
Negative regulators of DDX58/IFIH1 signaling	9.14E-03	67.65
Regulation of cholesterol biosynthesis by SREBP (SREBF)	2.93E-03	61.82
Semaphorin interactions	3.77E-04	61.54
ER-Phagosome pathway	3.25E-05	60.47
[a]*Antigen processing-Cross presentation, cytokine signaling in Immune system, adaptive & innate immune system, signaling by interleukins*		
Amplification of signal from the kinetochores	3.73E-06	60.42
Signaling by PTK6	4.34E-02	57.41
Signaling by VEGF	4.42E-05	57.01
Oxygen-dependent proline hydroxylation of Hypoxia-inducible Factor Alpha	2.14E-02	56.06
Costimulation by the CD28 family	1.96E-02	55.71
Death Receptor Signaling	3.71E-02	47.55
Apoptosis	1.35E-02	46.63
DNA Repair	1.80E-03	43.99
Cellular responses to external stimuli	6.47E-06	43.50
Cellular responses to stress	3.11E-04	42.92
Adaptive Immune System	3.82E-07	41.99
Membrane Trafficking	1.74E-03	40.22

[a] Subterms relevant to immune parameters in italics.

Table 6
Biological process enrichment terms for 1 μM sodium arsenite treatment.

Go Term	Term p-value	% Genes	Associated Genes Found
Regulation of interleukin-2 production	6.60E-04	6.76	[ANXA1, CD4, IL17 F, LAG3, PDE4D]
Regulation of viral genome replication	5.67E-04	5.04	[ADAR, EIF2AK2, ISG15, MX1, OAS1, ZC3HAV1]
Interferon-gamma production	1.89E-06	6.29	[BTN3A1, BTN3A2, BTN3A3, HLA-A, HLA-DPA1, HLA-DPB1, IL18RAP, ISG15, PDE4D, SLAMF6]
Alpha-beta T cell activation	2.81E-06	5.95	[ANXA1, BCL11B, BCL6, HLA-A, IFNG, RORC, SLAMF6, TCF7, TNFRSF14, TNFSF8]
Positive regulation of hemopoiesis	1.17E-06	5.06	[ANXA1, BCL6, CD4, ETS1, FLI1, HLA-G, ID2, IFNG, IL17A, IL7R, ISG15, LIF]
Type I interferon signaling pathway	3.44E-13	13.21	[ADAR, HLA-A, HLA-B, HLA-C, HLA-F, HLA-G, HLA-H, ISG15, MX1, OAS1, OAS2, PSMB8, SP100, USP18]

Table 7
Reactome pathway enrichment terms for 1 μM sodium arsenite treatment.

Go Term	Term p-value	% Genes	Associated Genes Found
TNFs bind their physiological receptors	1.50E-02	10.34	[TNFRSF14, TNFRSF8, TNFSF8]
Interleukin-4 and Interleukin-13 signaling	5.03E-06	8.33	[ANXA1, BCL6, HMOX1, IL17A, IL17 F, LIF, OPRM1, OSM, RORC]
Butyrophilin (BTN) family interactions	1.75E-03	25.00	[BTN3A1, BTN3A2, BTN3A3]
Iron uptake and transport	1.32E-02	5.17	[FTH1, FTL, HMOX1]
Cytokine Signaling in Immune system	1.54E-19	5.35	[ADAR, ANXA1, B2M, BCL6, CD4, EIF2AK2, HLA-A, HLA-B, HLA-C, HLA-DPA1, HLA-DPB1, HLA-F, HLA-G, HMOX1, IFNG, IL17A, IL17 F, IL18RAP, IL7R, ISG15, LIF, MX1, OAS1, OAS2, OPRM1, OSM, PSMB8, PSMB9, PTPN13, RORC, SP100, SQSTM1, TALDO1, TNFRSF14, TNFRSF8, TNFSF8, USP18]
DAG and IP3 signaling	2.17E-02	7.14	[ADCY1, ITPR1, PRKCE]
ISG15 antiviral mechanism	1.72E-02	5.48	[EIF2AK2, ISG15, MX1, USP18]
Vpu mediated degradation of CD4	1.97E-02	5.77	[CD4, PSMB8, PSMB9]
Antiviral mechanism by IFN-stimulated genes	9.52E-04	7.41	[EIF2AK2, ISG15, MX1, OAS1, OAS2, USP18]

and DNA repair".

DEGs that were due to alterations in activation by 1 μM sodium arsenite treatment were analyzed for significantly enriched biological process and Reactome pathways. There were 6 leading biological process terms identified as being enriched (Table 6). The leading terms identified at the lower sodium arsenite dose include: "regulation of IL-2 production, regulation of viral genome replication, IFNγ production, α/β T-cell activation, positive regulation of hemopoiesis and type I interferon signaling" (Table 6), all significantly enriched leading group terms, sub-terms and genes are listed in Supplemental Table 6. All of the significantly enriched biological terms identified with the 1 μM sodium arsenite treatment were related to immune system processes (Table 6

Table 8
Biological process enrichment terms for 1 μM sodium arsenite +3 μM uranyl acetate treatment.

Go Term	Term p-value	% Genes	Associated Genes Found
Positive regulation of phosphatase activity	1.18E-04	9.80	[CALM3, IFNG, **PICALM, PTPRC, SMAD3**]
Regulation of viral genome replication	9.40E-04	5.04	[ADAR, EIF2AK2, MX1, OAS1, **OAS3**, ZC3HAV1]
Embryonic cranial skeleton morphogenesis	1.42E-04	9.43	[**AUTS2, CHST11, SMAD3**, SQSTM1, **TGFBR2**]
Interferon-gamma production	2.06E-05	5.66	[BTN3A1, BTN3A2, BTN3A3, HLA-A, HLA-DPA1, IL18RAP, **PDE4B**, PDE4D, SLAMF6]
Regulation of interleukin-2 production	6.30E-06	9.46	[ANXA1, CD4, IL17 F, LAG3, **PDE4B**, PDE4D, **PTPRC**]
Polyol metabolic process	3.84E-05	5.23	[**CALM3, DHX8**, IFNG, **INPP4B, IP6K1, ITPKB, MECP2, PICALM, SPTLC2**]
Cellular iron ion homeostasis	2.38E-04	6.52	[**CALM3**, FTH1, FTL, HMOX1, **PICALM**, **SOD1**]
Leukocyte homeostasis	9.40E-04	5.04	[ANXA1, **ITPKB, PDE4B**, PMAIP1, SQSTM1, **TSC22D3**]
Myeloid cell homeostasis	6.49E-10	7.58	[ANXA1, B2M, BCL6, ETS1, FLI1, HMOX1, ID2, **IKZF1**, **ITPKB**, **KMT2E**, **MED1, PDE4B, PRDX1, SOD1, YWHAQ**]
CD4-positive, alpha-beta T cell differentiation involved in immune response	4.59E-04	7.35	[ANXA1, BCL6, IFNG, RORC, SLAMF6]
Regulation of cell killing	2.52E-12	12.61	[B2M, HLA-A, HLA-B, HLA-C, **HLA-E**, HLA-F, HLA-H, IFNG, IL18RAP, IL7R, LAG3, LAMP1, **PTPRC**, SLAMF6]

and Supplemental Table 6) reinforcing the observation that lower sodium arsenite doses may target T-cell activation.

Retention of the significant differential expression of the human leukocyte antigen (HLA) genes including *HLA–A*, *B*, *C*, *F*, *G*, *H* and *HLADPA1*, *HLADPB1* were key to the enrichment of leading biological process terms "IFNγ production and type I interferon signaling". Four of the significantly enriched biological terms identified at the lower 1 μM sodium arsenite dose did not rely on the enrichment of the *HLA* DEGs including "regulation of IL-2 production, regulation of viral genome replication, α/β T-cell activation and positive regulation of hemopoiesis" (Table 6).

There were 9 leading enriched Reactome pathway terms (highest p value and % genes per term) identified at the lower 1 μM sodium arsenite dose (Table 7), all significantly enriched leading group terms, subterms and genes are listed in Supplemental Table 7. Eight of the leading enriched pathways modulate T-cell activation including "Interleukin-4 and Interleukin-13 signaling, cytokine signaling in immune system, DAG and IP3 signaling and butyrophilin (BTN) family interactions". The only non-immune cellular process pathway enriched with the 1 μM sodium arsenite treatment involved "iron uptake and transport".

One hundred and two genes were altered by both the 1 μM sodium arsenite and 1 μM sodium arsenite + 3 μM uranyl acetate treatments. Eighty-nine genes were significantly altered by only the mixture. DEGs that were due to alterations in activation by the mixture (1 μM sodium arsenite and 3 μM uranyl acetate compared to activated) were analyzed for significantly enriched biological process and Reactome pathways. By adding uranyl acetate to the low dose sodium arsenite treatment an additional 5 biological process terms were identified as being enriched (Table 8). When a biological term contained ≥50 % of the 89 genes significantly altered by only the mixture, the term and genes were bolded (Table 8), 6 of the enriched biological process terms and 2 of the Reactome pathways were more influenced by the 89 genes significantly altered by the mixture compared to those by the arsenic alone. Leading terms, sub-terms and genes enriched in those terms are listed in Supplemental Table 8. In addition to the immune pathways modified by the 1 μM sodium arsenite treatment, adding uranyl acetate altered biological processes related to glucose metabolism, regulation of cell killing, phosphatase activity and regulation of sequestered calcium.

There were 11 leading enriched Reactome pathway terms 1 μM sodium arsenite and 3 μM uranyl acetate treatment (highest p value and % genes per term) identified (Table 9). When a Reactome pathway term contained ≥50 % of the 89 genes significantly altered by only the mixture, the term and genes were bolded (Table 9). Sub-terms with a lower *p*-value that were organized under a leading pathway term and were associated with T-cell activation and/or the immune response are listed in italics under the leading Reactome pathway term (Supplemental Table 9). Adding uranyl acetate altered additional immune pathways including "detoxification of reactive oxygen species,

Table 9
Reactome pathway enrichment terms for 1 μM sodium arsenite +3 μM uranyl acetate treatment.

Go Term	Term p-value	% Genes	Associated Genes Found
Detoxification of Reactive Oxygen Species	2.05E-03	13.51	[GSTP1, PRDX1, SOD1, TXN, TXNRD1]
Interleukin-4 and Interleukin-13 signaling	1.36E-04	8.33	[ANXA1, BCL6, HMOX1, IL17 F, LIF, OPRM1, OSM, **POU2F1**, RORC]
Butyrophilin (BTN) family interactions	8.64E-03	25.00	[BTN3A1, BTN3A2, BTN3A3]
Transcriptional regulation by RUNX3	3.79E-03	7.22	[**BRD2**, CREBBP, PSMB8, PSMB9, RORC, **SMAD3**, TCF7]
OAS antiviral response	3.85E-03	33.33	[OAS1, OAS2, **OAS3**]
Cytokine Signaling in Immune system	1.62E-13	5.21	[ADAR, ANXA1, B2M, BCL6, CD4, EIF2AK2, HLA-A, HLA-B, HLA-C, HLA-DPA1, **HLA-E**, HLA-F, HMOX1, IFNG, IL17 F, IL18RAP, IL7R, LIF, MX1, OAS1, OAS2, **OAS3**, OPRM1, OSM, **POU2F1**, PSMB8, PSMB9, PTPN13, RORC, **SMAD3, SOD1**, SP100, SQSTM1, TALDO1, TNFRSF8, TNFSF8]
Phosphorylation of CD3 and TCR zeta chains	4.61E-02	13.64	[CD4, HLA-DPA1, **PTPRC**]
Uptake and function of anthrax toxins	2.05E-02	18.75	[ANTXR2, **CALM3**, FURIN]
Degradation of GLI2 by the proteasome	3.12E-02	5.00	[**CSNK1A1**, PSMB8, PSMB9]
RORA activates gene expression	2.73E-02	16.67	[**CREBBP, MED1**, NCOA2]
FOXO-mediated transcription	3.21E-03	9.23	[BCL6, **CREBBP, SMAD3**, TXN, TXNIP, **YWHAQ**]
ER-Phagosome pathway	2.08E-05	10.47	[B2M, HLA-A, HLA-B, HLA-C, **HLA-E**, HLA-F, PSMB8, PSMB9, TAP1]

Table 10
Mean Log 2 fold-change of RNA sequencing vs PCR validation of select genes for Donor 1.

				Relative to Activated		
Gene Name	Ensembl ID	Detection Method	Activated	1 μM NaAs	10 μM NaAs	1 μM NaAs + 3 μM UA
HMOX1	ENSG00000100292.17	RNA Seq	1.34 ± 0.54	4.62 ± 0.36	8.80 ± 0.36	4.68 ± 0.36
		PCR	1.41 ± 0.13	5.15 ± 0.46	9.33 ± 0.20	6.01 ± 0.58
NQO1	ENSG00000181019.13	RNA Seq	2.18 ± 0.29	0.77 ± 0.19	1.88 ± 0.18	0.78 ± 0.20
		PCR	0.85 ± 0.14	1.38 ± 0.41	2.21 ± 0.27	1.66 ± 0.43
IFNG	ENSG00000111537.5	RNA Seq	10.55 ± 0.47	−0.59 ± 0.10	−3.58 ± 0.11	−0.41 ± 0.10
		PCR	9.03 ± 0.32	−0.09 ± 0.40	−2.94 ± 0.23	0.53 ± 0.32
IL2	ENSG00000109471.5	RNA Seq	5.9 ± 0.85	−0.28 ± 0.71	1.29 ± 0.71	0.14 ± 0.71
		PCR	4.85 ± 0.42	0.31 ± 0.46	1.59 ± 0.18	1.02 ± 0.60
FZD4	ENSG00000174804.4	RNA Seq	4.54 ± 0.93	−2.09 ± 0.58	−5.71 ± 1.26	−3.42 ± 0.86
		PCR	4.78 ± 0.24	−1.96 ± 0.38	−6.48 ± 0.45	−1.29 ± 0.50
CTLA4	ENSG00000163599.17	RNA Seq	6.15 ± 0.15	−0.17 ± 0.09	−3.13 ± 0.10	−0.19 ± 0.09
		PCR	4.25 ± 0.47	0.17 ± 0.37	−1.64 ± 1.65	0.1 ± 0.82
CMPK2	ENSG00000134326.11	RNA Seq	2.29 ± 0.41	−1.14 ± 0.40	−0.82 ± 0.40	−1.45 ± 0.41
		PCR	0.85 ± 0.49	−0.83 ± 0.40	−1.25 ± 0.33	−0.06 ± 0.46
OAS3	ENSG00000111331.13	RNA Seq	1.95 ± 0.30	−0.88 ± 0.30	0.10 ± 0.29	−0.99 ± 0.30
		PCR	0.55 ± 0.53	−0.14 ± 0.15	0.37 ± 0.33	0.46 ± 0.79

Abbreviations: NaAs, sodium arsenite; UA, uranyl acetate Results based on RNA obtained from donor 1.

phosphorylation of CD3 and TCR zeta chains, RORA activates gene transcription and the FOXO-mediated transcription" pathways. Seven of the leading enriched pathways modulate T-cell activation. The non-immune related Reactome pathway most affected by the addition of uranyl acetate is the detoxification of reactive oxygen species due to the genes thioredoxin (*TXN*), thioredoxin reductase 1 (*TXNRD1*) and thioredoxin-interacting protein (*TXNIP*) and the "uptake and actions of bacterial toxins".

3.6. PCR validation

We selected 8 genes for PCR validation that were altered due to T-cell activation or metal treatment. Table 10 compares the Log 2 fold-changes from the RNA sequencing and PCR validation for donor 1. Results showed that changes between activation and activation in the presence of 10 μM sodium arsenite induced large increases in gene expression in markers of oxidative stress including *HMOX1* and *NQO1*. These markers were also increased with the 1 μM sodium arsenite and 1 μM sodium arsenite + 3 μM uranyl acetate treatments and fold changes were comparable between the two techniques. Markers of T-cell activation showed consistent increases with activation and decreases in the presence of 10 μM sodium arsenite including *IFNG*, *FZD4* and *CTLA4*. Differences in the magnitude change detected by RNA sequencing and PCR did exist for the T-cell activation markers. Spearman's rank correlation comparing RNA sequencing and corresponding PCR log 2 fold-change values for the unactivated CD4+ T-cells vs activated alone ($r = 0.7$, $p = 0.59$), activated vs 10 μM sodium arsenite ($r = 1$, $p = <0.0001$), 1 μM sodium arsenite ($r = 0.97$, $p = 0.004$) and 1 μM sodium arsenite + 3 μM uranyl acetate ($r = 0.92$, $p = 0.002$) showed significant correlation between the two techniques. Changes due to metal treatment for these 8 genes were assessed by PCR using human CD4+ T-cells from two additional donors, one male and one female. Supplemental Table 10 compares the Log 2 fold-changes from the RNA sequencing for donor 1 and the PCR validation for all donors. Though variation exists, there were consistent trends between the multiple donors.

4. Discussion

This study presents a comprehensive analysis of global gene expression changes in response to an environmentally relevant dose and form of sodium arsenite in the presence and absence of uranium. U.S. Geological Survey data reports that 0.92 % of sodium arsenite groundwater concentrations sampled nationally exceed 50 μg/L, however regionally in the southwest that percentage ranges from 0.35 to 2.2 % [43]. Credo et al. [44] reported that in ground water samples from the western portion of the Navajo Nation, arsenic concentrations ranged from 0.03 to 190 ug/L and uranium ranged from 0.04 to 490 μg/L. Uranium levels in waterways adjacent to the Jackpile mine in Laguna Pueblo measured as high as 772 μg/L [6]. The amount of atomic arsenic and uranium at the lower treatment conditions tested in this study fall within these environmental ranges [1 μM sodium arsenite = 129.91 μg/L NaAs or 74.92 μg/L As, 3 μM uranyl acetate = 1272.4 μg/L UA or 713.81 μg/L U]. Uranium and arsenic can co-occur as contaminants in water sources near AUMs in the Western United States and are a health concern in impacted communities that rely on unregulated water sources. In this study, we demonstrate that sodium arsenite, in the absence of uranyl acetate, induces a dose-dependent alteration in the magnitude of gene expression associated with both activation and differentiation following CD3/CD28 activation of CD4+ T-cells. While fewer genes were significantly affected at the lower sodium arsenite concentration (1 μM), biological process and pathway analysis revealed that alterations to oxidative stress and immune function signatures were observed. Importantly, although uranyl acetate alone did not alter gene expression, the combination of low dose uranyl acetate (3 μM) and low dose sodium arsenite (1 μM) resulted in differential changes in gene expression compared to

the effects of low dose sodium arsenite alone, indicating a possible mixed metal effect.

One of the known mechanisms of arsenic toxicity is the ability to generate oxidative stress in cells and tissues. Metal-induced oxidative stress has been shown to be an underlying cause of metal toxicity [45–48] and can modify gene expression, directly induce DNA damage and lipid peroxidation and cause protein modification [49]. As reviewed in Franchina et al. [50], a certain level of oxidative stress is required for full TCR activation and plays a role in differentiation, however oxidative stress above this level could perturb TCR activation leading to immune dysregulation. This study shows that alterations in oxidative stress genes are significantly upregulated in the presence of the higher (10 μM) sodium arsenite dose with increases in *HMOX1*, *NQO1* and *GCLM* retained at the lower (1 μM) sodium arsenite dose (Table 3). This lower dose effect is consistent with results in the literature [23,30]. Consistent with our findings significant alterations in T-cell activation occur with arsenic [23,25,29].

The expression of activation/costimulation markers *IFNG*, *LAG3*, *ICOS*, and *CTLA4* as well as 2 of the trimeric IL2 receptor subunits, *IL2RA* and *IL2RB* was decreased in the presence of 10 μM sodium arsenite. Decreases in *LAG3* and *IFNG* expression were observed in the presence of 1 μM sodium arsenite but to a lesser degree.

CD4+ T-cells activated in the presence of 10 μM sodium arsenite had an increased expression of *IL2*, *CD69* and *TNFA*. The IL-2 signaling axis plays a pivotal role in T-cell activation and differentiation by promoting cellular proliferation, determining subtype and stimulating T-cells to synthesize more IL-2 and IFNγ. Increased IL-2 signaling promotes Th1 and Th2 cell differentiation and suppresses differentiation of the Th-17 lineage promoting immune-stimulation [51], while low IL-2 levels promote T-regulatory lineage and immune-suppression. In our study, we observe an increased *IL2* expression with the higher and a decrease in *IL2* expression in the presence of the lower sodium arsenite dose. Others have described an increase in *IL2* expression with 1 μM arsenic pre-treatment after 72 h of activation with PHA whereas a decrease in *IL2* expression is observed in cells treated with similar concentrations of arsenic but for shorter time periods [23,25,29]. These data suggest that *IL2* expression is a sensitive target for arsenic and differing pre-treatment times, concentrations & forms may account for the mixed results in the literature.

Selected Th1 and Th17 differentiation markers were significantly altered in the presence of the higher dose sodium arsenite treatment and decreased expression of *IFNG* and *IL17A* was observed even at the lower dose (Table 2), suggesting a mechanism for sodium arsenite-induced immune dysregulation. IFNɣ is produced primarily by activated T-cells and activates macrophages, increases antigen presentation and induction of MHC-peptide complexes, regulates T-cell polarization and increases antiviral immunity [52]. Suppression of *IFNG* has been reported with arsenic treatment *in vitro* [30]. Additionally, exposure studies have also reported decreased IFNɣ in people exposed to arsenic through coal burning [53] and in people with arsenic induced skin lesions [22]. Th17 cells readily express *IL17A* and are important for the protection against extracellular microbes [54]. A suppression of Th1 or Th17 cells differentiation and/or a reduction in subsequent cytokines may increase susceptibility to intracellular bacterial and viral infections.

Previous research demonstrates that uranium exposures in populations and in cell culture models can alter immune parameters including T-cell subtype counts and the expression of a number of cytokines, suggesting uranium may interfere with TCR activation [18,20,26]. In our study, activation of CD4+ T-cells with CD3/CD28 in the presence of uranyl acetate alone did not impact the expression changes of any genes. This is in contrast to previous reports that uranium induced gene expression changes in murine CD4+ T-cells, albeit at a concentration of 100 μM (3-times the highest concentration used in this study) [20]. Additionally, uranium has been reported to promote oxidative stress in human lymphocytes, however millimolar concentrations of uranium were used [55]. Previous research from our lab demonstrates that uranyl acetate did not induce oxidative stress in an immortalized T-cell line (Jurkat cells) at similar concentrations used in this study [42]. One may argue that uranyl ions are large molecules and our observed results are due to the molecules being unable to readily enter in the cells. However, research supports that uranyl ion molecules are able to enter cell types including human liver cancer cells (HEPG2) cells, Jurkat human T-lymphocytic clone E6.1 (Jurkat), THP-1 human monocytic cells and human neuroblastoma cells (SH-SY5Y) [42,56,57].

When lower doses of sodium arsenite and uranyl acetate were combined to replicate an environmentally relevant exposure mixture, combined effects led to significant gene expression changes in an additional 89 genes compared to low dose sodium arsenite alone. Changes in DEGs with the mixture are novel and may be meaningful. Based on the biological processes and Reactome pathways that were enriched with

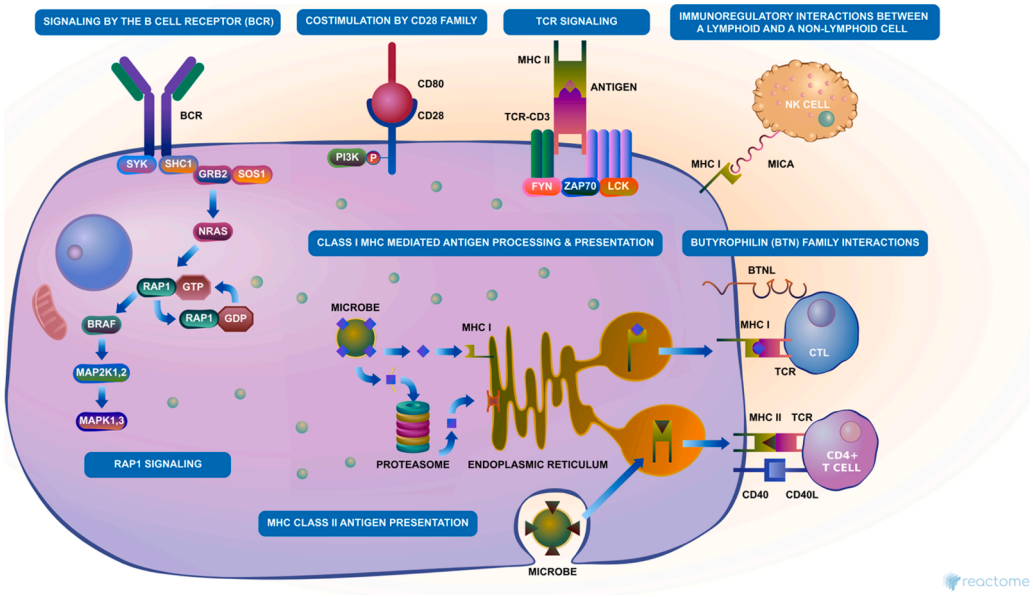

Fig. 4. Adaptive immune diagram of Reactome pathways altered by metal mixture. The 191 DEGs for the 1 μM sodium arsenite and 3 μM uranyl acetate were input into the Reactome analysis tool. The immune system subcategory adaptive immune response was magnified to show pathways influenced by the mixture.

the mixture, interactions between sodium arsenite and uranyl acetate may target "RORA activates gene expression" and "FOXO-mediated transcription" Reactome pathways as well as the "Polyol metabolic process" biological term. The "FOXO-mediated transcription" pathway is activated in response to environmental changes such as oxidative stress, and incorporates signaling networks that regulate cell survival, growth, differentiation and metabolism. RORγt, and to a lesser extent, RORα act in concert during Th17 development and differentiation. The "RORA activates gene expression" pathway is further enriched when uranyl acetate is added to sodium arsenite treatment. Uranyl acetate in combination with sodium arsenite enriches the "RORA activates gene expression" and "FOXO-mediated transcription" pathways which are involved in CD4+ differentiation suggesting that the metalloid mixture may influence CD4+ T-cell differentiation compared to each metal alone. Uranyl acetate in the presence of sodium arsenite enriched the biological term "Polyol metabolic process" which is a metabolic pathway reducing glucose activated when intracellular glucose concentrations are elevated. Alterations in glucose metabolism pathways may alter the survival and differentiation of the T-cells modulating the adaptive immune responses [58]. Nine of the 14 genes enriched in the Reactome pathways modulated by the mixture (bolded in Table 9) are represented in the adaptive immune enhanced high-level diagram generated by the Reactome analysis tool (Fig. 4), illustrating possible targeted pathways of the metal mixture [35,59]

PCR validation of the 8 selected genes was completed using RNA collected from all 3 donors. As expected variability in the PCR results between donors existed however, certain trends held up between donors (Supplemental Table 10). Activation alone elicited changes in the gene expression of the activation markers used in the study for all 3 donors demonstrating complete activation occurred. All 3 donors showed a dose dependent decrease in *IFNG*, *FZD4* and *CTLA4* due to high dose sodium arsenite treatment. Additionally, sodium arsenite induced a dose dependent increase in the oxidative stress marker *HMOX1*. Of importance to note is that uranyl acetate treatment alone did not significantly alter the expression of in the selected genes from any of the 3 donors tested, indicating that uranyl acetate alone may not exert a direct effect on gene expression at the doses used but may only show an effect in combination with other metals. Previous studies in animal models suggest that uranyl acetate has little impact on CD4+ T-cells [60] and that uranyl acetate is not cytotoxic or able to induce oxidative stress or DNA damage in Jurkat T-cells [42], supporting the lack of gene expression changes observed by uranyl acetate treatment in our study. Less variability was observed between donor 1 and donor 3 where in most genes the directionality of results was similar with slightly different magnitudes. Based on the results the response of donor 1 was not unique however the trends revealed in the PCR results will need to be investigated in a larger population of individuals.

The work presented in this study provides evidence that sodium arsenite and uranyl acetate together act differently on TCR activation compared to each metal alone. The results indicate that while uranyl acetate alone did not significantly alter global gene expression during T-cell activation in a controlled experimental system, changes in biological processes and pathways involved in T-cell activation and immune response are induced when in the presence of both low dose sodium arsenite and the mixture. This is supported by results indicating no alterations in T-cell subsets or function in mice exposed to uranium for 60 days [60]. In contrast, there is evidence indicating that populations exposed to uranium exhibit altered immune cell counts and function [16,19,26]. One important consideration is that very rarely are individuals and populations exposed to a single metal toxicant; exposures are more likely to be in the form of metal mixtures. The findings from this study demonstrate that exposures to metal mixtures of arsenic and uranium may result in meaningful differences in gene expression that could ultimately account, at least in part, for the observed uranium-associated immune dysregulation in human populations. These findings could inform future risk assessment studies of metal mixtures allowing for more accurate adverse effect assessment in exposed populations [61]. The full scope of the RNA sequencing analysis is limited to one donor however trends and differences present in the multiple donors suggests that full RNA sequencing analysis with a larger number of donors will reveal broader implications on the functional relevance of mixed metal-induced gene expression changes. This study reveals the need for further investigations on the impacts of environmentally relevant metal mixtures.

Data availability

No data was used for the research described in the article.
Data will be made available on request.

Author contributions

Jodi R. Schilz: Conceptualization; Data curation; Formal analysis; Funding acquisition; Investigation; Methodology; Visualization; Writing - original draft; Writing - review & editing. **Erica J. Dashner-Titus**: Conceptualization; Data curation; Formal analysis; Funding acquisition; Investigation; Methodology; Visualization; Writing - original draft; Writing - review & editing. **Li Luo:** Formal analysis; Software; Visualization; Writing – review & editing. **Karen A. Simmons**: Investigation; Validation. **Debra A. MacKenzie**: Resources; Writing – review & editing. **Laurie G. Hudson**: Project administration; Resources; Supervision; Writing - review & editing.

Funding sources

This work was funded by National Institutes of Health [P42 ES025589, 2017; P50 ES026102, 2015; P30 CA118100, 2005] www.nih.gov and the US Environmental Protection Agency [83615701, 2015], www.epa.gov. Training support for Dr. Dashner-Titus was provided by University of New Mexico Comprehensive Cancer center [P30 CA118100, 2005]. The funders had no role in study design, data collection and analysis, decision to publish, or preparation of the manuscript.

Conflict of Interest

The authors declare no conflict of interest.

Declaration of Competing Interest

The authors report no declarations of interest.

Acknowledgements

We would like to extend our gratitude to the staff at the National Center for Genome Resources (NCGR) for their help completing RNA Sequencing of our samples and to Sandra Alvarez for her help with the initial RNA sequencing analysis.

Appendix A. Supplementary data

Supplementary material related to this article can be found, in the online version, at doi:https://doi.org/10.1016/j.toxrep.2021.11.019.

References

[1] J.M. Blake, S. Avasarala, K. Artyushkova, A.-M.S. Ali, A.J. Brearley, C. Shuey, Wm. P. Robinson, C. Nez, S. Bill, J. Lewis, C. Hirani, J.S.L. Pacheco, J.M. Cerrato, Elevated concentrations of U and co-occurring metals in abandoned mine wastes in a northeastern Arizona Native American Community, Environ. Sci. Technol. 49 (2015) 8506–8514, https://doi.org/10.1021/acs.est.5b01408.

[2] J.M. Blake, S. Avasarala, A.-M.S. Ali, M. Spilde, J.S. Lezama-Pacheco, D. Latta, K. Artyushkova, A.G. Ilgen, C. Shuey, C. Nez, J.M. Cerrato, Reactivity of As and U

co-occurring in mine wastes in northeastern Arizona, Chem. Geol. 522 (2019) 26–37, https://doi.org/10.1016/j.chemgeo.2019.05.024.
[3] L. Corlin, T. Rock, J. Cordova, M. Woodin, J.L. Durant, D.M. Gute, J. Ingram, D. Brugge, Health effects and environmental justice concerns of exposure to uranium in drinking water, Curr. Environ. Health Rep. 3 (2016) 434–442, https://doi.org/10.1007/s40572-016-0114-z.
[4] J. Hoover, M. Gonzales, C. Shuey, Y. Barney, J. Lewis, Elevated arsenic and uranium concentrations in unregulated water sources on the Navajo Nation, USA, Expo. Health. 9 (2017) 113–124, https://doi.org/10.1007/s12403-016-0226-6.
[5] P.L. Toccalino, J.E. Norman, J.C. Scott, Chemical mixtures in untreated water from public-supply wells in the U.S.–occurrence, composition, and potential toxicity, Sci. Total Environ. 431 (2012) 262–270, https://doi.org/10.1016/j.scitotenv.2012.05.044.
[6] J.M. Blake, C.L. De Vore, S. Avasarala, A.-M. Ali, C. Roldan, F. Bowers, M.N. Spilde, K. Artyushkova, M.F. Kirk, E. Peterson, L. Rodriguez-Freire, J.M. Cerrato, Uranium mobility and accumulation along the Rio Paguate, Jackpile Mine in Laguna pueblo, NM, Environ. Sci. Process. Impacts 19 (2017) 605–621, https://doi.org/10.1039/C6EM00612D.
[7] E.J. Dashner-Titus, J. Hoover, L. Li, J.-H. Lee, R. Du, K.J. Liu, M.G. Traber, E. Ho, J. Lewis, L.G. Hudson, Metal exposure and oxidative stress markers in pregnant Navajo Birth Cohort Study participants, Free Radic. Biol. Med. 124 (2018) 484–492, https://doi.org/10.1016/j.freeradbiomed.2018.04.579.
[8] A. Asic, A. Kurtovic-Kozaric, L. Besic, L. Mehinovic, A. Hasic, M. Kozaric, M. Hukic, D. Marjanovic, Chemical toxicity and radioactivity of depleted uranium: the evidence from in vivo and in vitro studies, Environ. Res. 156 (2017) 665–673, https://doi.org/10.1016/j.envres.2017.04.032.
[9] N. Bellamri, C. Morzadec, O. Fardel, L. Vernhet, Arsenic and the immune system, Curr. Opin. Toxicol. 10 (2018) 60–68, https://doi.org/10.1016/j.cotox.2018.01.003.
[10] D. Brugge, V. Buchner, Health effects of uranium: new research findings, Rev. Environ. Health 26 (2011) 231–249.
[11] S.J.S. Flora, Arsenic-induced oxidative stress and its reversibility, Free Radic. Biol. Med. 51 (2011) 257–281, https://doi.org/10.1016/j.freeradbiomed.2011.04.008.
[12] A. Dustov, G. Mirojov, M. Yakubova, S. Umarov, D. Ishankulova, M. Eliasziw, D. Brugge, Uranium mine proximity, immune function, and Helicobacter pylori infection in Tajikistan, J. Toxicol. Environ. Health A. 76 (2013) 1261–1268, https://doi.org/10.1080/15287394.2013.836694.
[13] L. Hund, E.J. Bedrick, C. Miller, G. Huerta, T. Nez, S. Ramone, C. Shuey, M. Cajero, J. Lewis, A Bayesian framework for estimating disease risk due to exposure to uranium mine and mill waste on the Navajo Nation, J. R. Stat. Soc. Ser. A Stat. Soc. 178 (2015) 1069–1091, https://doi.org/10.1111/rssa.12099.
[14] M.E. Harmon, J. Lewis, C. Miller, J. Hoover, A.-M.S. Ali, C. Shuey, M. Cajero, S. Lucas, K. Zychowski, B. Pacheco, E. Erdei, S. Ramone, T. Nez, M. Gonzales, M. J. Campen, Residential proximity to abandoned uranium mines and serum inflammatory potential in chronically exposed Navajo communities, J. Expo. Sci. Environ. Epidemiol. 27 (2017) 365–371, https://doi.org/10.1038/jes.2016.79.
[15] J. Lewis, J. Hoover, D. MacKenzie, Mining and environmental health disparities in native American communities, Curr. Environ. Health Rep. 4 (2017) 130–141, https://doi.org/10.1007/s40572-017-0140-5.
[16] E. Erdei, C. Shuey, B. Pacheco, M. Cajero, J. Lewis, R.L. Rubin, Elevated autoimmunity in residents living near abandoned uranium mine sites on the Navajo Nation, J. Autoimmun. 99 (2019) 15–23, https://doi.org/10.1016/j.jaut.2019.01.006.
[17] N.L. Dangleben, C.F. Skibola, M.T. Smith, Arsenic immunotoxicity: a review, Environ. Health Glob. Access Sci. Source. 12 (2013) 73, https://doi.org/10.1186/1476-069X-12-73.
[18] Y. Hao, J. Ren, J. Liu, Z. Yang, C. Liu, R. Li, Y. Su, Immunological changes of chronic oral exposure to depleted uranium in mice, Toxicology 309 (2013) 81–90, https://doi.org/10.1016/j.tox.2013.04.013.
[19] S.E. Wagner, J.B. Burch, M. Bottai, S.M. Pinney, R. Puett, D. Porter, J.E. Vena, J. R. Hébert, Hypertension and hematologic parameters in a community near a uranium processing facility, Environ. Res. 110 (2010) 786–797, https://doi.org/10.1016/j.envres.2010.09.004.
[20] B. Wan, J.T. Fleming, T.W. Schultz, G.S. Sayler, In vitro immune toxicity of depleted uranium: effects on murine macrophages, CD4+ T cells, and gene expression profiles, Environ. Health Perspect. 114 (2006) 85–91.
[21] M. Scammell, C. Sennett, R. Laws, R. Rubin, D. Brooks, J. Amador, D. López-Pilarte, O. Ramirez-Rubio, D. Friedman, M. McClean, Navajo Birth Cohort Study Team, J. Lewis, E. Erdei, Urinary metals concentrations and biomarkers of autoimmunity among Navajo and nicaraguan men, Int. J. Environ. Res. Public Health 17 (2020) 5263, https://doi.org/10.3390/ijerph17155263.
[22] R. Biswas, P. Ghosh, N. Banerjee, J. Das, T. Sau, A. Banerjee, S. Roy, S. Ganguly, M. Chatterjee, A. Mukherjee, A. Giri, Analysis of T-cell proliferation and cytokine secretion in the individuals exposed to arsenic, Hum. Exp. Toxicol. 27 (2008) 381–386, https://doi.org/10.1177/0960327108094607.
[23] K.R. VanDenBerg, R.A. Freeborn, S. Liu, R.C. Kennedy, J.W. Zagorski, C. E. Rockwell, Inhibition of early T cell cytokine production by arsenic trioxide occurs independently of Nrf2, PLoS One 12 (2017), https://doi.org/10.1371/journal.pone.0185579 e0185579.
[24] R. Gera, V. Singh, S. Mitra, A.K. Sharma, A. Singh, A. Dasgupta, D. Singh, M. Kumar, P. Jagdale, S. Patnaik, D. Ghosh, Arsenic exposure impels CD4 commitment in thymus and suppress T cell cytokine secretion by increasing regulatory T cells, Sci. Rep. 7 (2017) 7140, https://doi.org/10.1038/s41598-017-07271-z.
[25] C. Morzadec, F. Bouezzedine, M. Macoch, O. Fardel, L. Vernhet, Inorganic arsenic impairs proliferation and cytokine expression in human primary T lymphocytes, Toxicology 300 (2012) 46–56, https://doi.org/10.1016/j.tox.2012.05.025.
[26] J. Lourenço, R. Pereira, F. Pinto, T. Caetano, A. Silva, T. Carvalheiro, A. Guimarães, F. Gonçalves, A. Paiva, S. Mendo, Biomonitoring a human population inhabiting nearby a deactivated uranium mine, Toxicology 305 (2013) 89–98, https://doi.org/10.1016/j.tox.2013.01.011.
[27] M. Barberis, T. Helikar, P. Verbruggen, Simulation of stimulation: cytokine dosage and cell cycle crosstalk driving timing-dependent T cell differentiation, Front. Physiol. 9 (2018) 879, https://doi.org/10.3389/fphys.2018.00879.
[28] C. Morzadec, M. Macoch, M. Robineau, L. Sparfel, O. Fardel, L. Vernhet, Inorganic arsenic represses interleukin-17A expression in human activated Th17 lymphocytes, Toxicol. Appl. Pharmacol. 262 (2012) 217–222, https://doi.org/10.1016/j.taap.2012.05.004.
[29] C. Martin-Chouly, C. Morzadec, M. Bonvalet, M.-D. Galibert, O. Fardel, L. Vernhet, Inorganic arsenic alters expression of immune and stress response genes in activated primary human T lymphocytes, Mol. Immunol. 48 (2011) 956–965, https://doi.org/10.1016/j.molimm.2011.01.005.
[30] C. Morzadec, M. Macoch, L. Sparfel, S. Kerdine-Römer, O. Fardel, L. Vernhet, Nrf2 expression and activity in human T lymphocytes: stimulation by T cell receptor activation and priming by inorganic arsenic and tert-butylhydroquinone, Free Radic. Biol. Med. 71 (2014) 133–145, https://doi.org/10.1016/j.freeradbiomed.2014.03.006.
[31] S. Anders, A. Reyes, W. Huber, Detecting differential usage of exons from RNA-Seq data, Nat. Preced. (2012), https://doi.org/10.1038/npre.2012.6837.2.
[32] M.I. Love, W. Huber, S. Anders, Moderated estimation of fold change and dispersion for RNA-seq data with DESeq2, Genome Biol. 15 (2014) 550, https://doi.org/10.1186/s13059-014-0550-8.
[33] J.R. Schilz, E.J. Dashner-Titus, L. Lou, K. Simmons, D.A. MacKenzie, L.G. Hudson, Co-exposure of Sodium Arsenite and Uranyl Acetate Differentially Alters Gene Expression in CD3/CD28 Activated CD4+ T-cells, 2020, https://doi.org/10.6073/pasta/f198331f536a56a696226405e4d9561f.
[34] G. Bindea, B. Mlecnik, H. Hackl, P. Charoentong, M. Tosolini, A. Kirilovsky, W.-H. Fridman, F. Pagès, Z. Trajanoski, J. Galon, ClueGO: a Cytoscape plug-in to decipher functionally grouped gene ontology and pathway annotation networks, Bioinforma. Oxf. Engl. 25 (2009) 1091–1093, https://doi.org/10.1093/bioinformatics/btp101.
[35] A. Fabregat, K. Sidiropoulos, G. Viteri, O. Forner, P. Marin-Garcia, V. Arnau, P. D'Eustachio, L. Stein, H. Hermjakob, Reactome pathway analysis: a high-performance in-memory approach, BMC Bioinformatics 18 (2017) 142, https://doi.org/10.1186/s12859-017-1559-2.
[36] B. Jassal, L. Matthews, G. Viteri, C. Gong, P. Lorente, A. Fabregat, K. Sidiropoulos, J. Cook, M. Gillespie, R. Haw, F. Loney, B. May, M. Milacic, K. Rothfels, C. Sevilla, V. Shamovsky, S. Shorser, T. Varusai, J. Weiser, G. Wu, L. Stein, H. Hermjakob, P. D'Eustachio, The reactome pathway knowledgebase, Nucleic Acids Res. 48 (2020) D498–D503, https://doi.org/10.1093/nar/gkz1031.
[37] M.V. Goldberg, C.G. Drake, LAG-3 in cancer immunotherapy, Curr. Top. Microbiol. Immunol. 344 (2011) 269–278, https://doi.org/10.1007/82_2010_114.
[38] C.H. June, J.A. Ledbetter, T. Lindsten, C.B. Thompson, Evidence for the involvement of three distinct signals in the induction of IL-2 gene expression in human T lymphocytes, J. Immunol. Baltim. Md 1950 143 (1989) 153–161.
[39] M. Wang, D. Windgassen, E.T. Papoutsakis, Comparative analysis of transcriptional profiling of CD3+, CD4+ and CD8+ T cells identifies novel immune response players in T-cell activation, BMC Genomics 9 (2008) 225, https://doi.org/10.1186/1471-2164-9-225.
[40] F.T. Lauer, F. Parvez, P. Factor-Litvak, X. Liu, R.M. Santella, T. Islam, M. Eunus, N. Alam, A.K.M.R. Hasan, M. Rahman, H. Ahsan, J. Graziano, S.W. Burchiel, Changes in human peripheral blood mononuclear cell (HPBMC) populations and T-cell subsets associated with arsenic and polycyclic aromatic hydrocarbon exposures in a Bangladesh cohort, PLoS One 14 (2019), https://doi.org/10.1371/journal.pone.0220451 e0220451.
[41] U.C. Nygaard, Z. Li, T. Palys, B. Jackson, M. Subbiah, M. Malipatlolla, V. Sampath, H. Maecker, M.R. Karagas, K.C. Nadeau, Cord blood T cell subpopulations and associations with maternal cadmium and arsenic exposures, PLoS One 12 (2017), https://doi.org/10.1371/journal.pone.0179606 e0179606.
[42] E.J. Dashner-Titus, J.R. Schilz, K.A. Simmons, T.R. Duncan, S.C. Alvarez, L. G. Hudson, Differential response of human T-lymphocytes to arsenic and uranium, Toxicol. Lett. 333 (2020) 269–278, https://doi.org/10.1016/j.toxlet.2020.08.013.
[43] ISSI Consulting Group, The Cadmus Group, Inc, ICF Consulting, Arsenic Occurrence in Public Drinking Water Supplies, 2000 (accessed May 13, 2020), https://nepis.epa.gov/Exe/ZyPURL.cgi?Dockey=P1004W96.txt.
[44] J. Credo, J. Torkelson, T. Rock, J.C. Ingram, Quantification of elemental contaminants in unregulated water across Western Navajo Nation, Int. J. Environ. Res. Public Health 16 (2019), https://doi.org/10.3390/ijerph16152727.
[45] M. Valko, K. Jomova, C.J. Rhodes, K. Kuča, K. Musílek, Redox- and non-redox-metal-induced formation of free radicals and their role in human disease, Arch. Toxicol. 90 (2016) 1–37, https://doi.org/10.1007/s00204-015-1579-5.
[46] M. Valko, D. Leibfritz, J. Moncol, M.T.D. Cronin, M. Mazur, J. Telser, Free radicals and antioxidants in normal physiological functions and human disease, Int. J. Biochem. Cell Biol. 39 (2007) 44–84, https://doi.org/10.1016/j.biocel.2006.07.001.
[47] K. Jomova, M. Valko, Advances in metal-induced oxidative stress and human disease, Toxicology. 283 (2011) 65–87, https://doi.org/10.1016/j.tox.2011.03.001.
[48] M. Hossein Asghari, S. Saeidnia, M. Amin Rezvanfar, M. Abdollahi, A systematic review of the molecular mechanisms of uranium -Induced reproductive toxicity,

Inflamm. Allergy-Drug Targets. 14 (2016) 67–76, https://doi.org/10.2174/1871528114666160105112441.
[49] M. Valko, K. Jomova, C.J. Rhodes, K. Kuča, K. Musílek, Redox- and non-redox-metal-induced formation of free radicals and their role in human disease, Arch. Toxicol. 90 (2016) 1–37, https://doi.org/10.1007/s00204-015-1579-5.
[50] D.G. Franchina, C. Dostert, D. Brenner, Reactive oxygen species: involvement in t cell signaling and metabolism, Trends Immunol. 39 (2018) 489–502, https://doi.org/10.1016/j.it.2018.01.005.
[51] S.H. Ross, D.A. Cantrell, Signaling and function of Interleukin-2 in t lymphocytes, Annu. Rev. Immunol. 36 (2018) 411–433, https://doi.org/10.1146/annurev-immunol-042617-053352.
[52] G. Tau, P. Rothman, Biologic functions of the IFN-gamma receptors, Allergy 54 (1999) 1233–1251, https://doi.org/10.1034/j.1398-9995.1999.00099.x.
[53] Q. Zeng, P. Luo, J. Gu, B. Liang, Q. Liu, A. Zhang, PKC θ-mediated Ca2+/NF-AT signalling pathway may be involved in T-cell immunosuppression in coal-burning arsenic-poisoned population, Environ. Toxicol. Pharmacol. 55 (2017) 44–50, https://doi.org/10.1016/j.etap.2017.08.005.
[54] W. Ouyang, J.K. Kolls, Y. Zheng, The biological functions of T helper 17 cell effector cytokines in inflammation, Immunity 28 (2008) 454–467, https://doi.org/10.1016/j.immuni.2008.03.004.
[55] M. Soltani, M.H. Zarei, A. Salimi, J. Pourahmad, Mitochondrial protective and antioxidant agents protect toxicity induced by depleted uranium in isolated human lymphocytes, J. Environ. Radioact. 203 (2019) 112–116, https://doi.org/10.1016/j.jenvrad.2019.03.009.
[56] Y. Guéguen, D. Suhard, C. Poisson, L. Manens, C. Elie, G. Landon, C. Bouvier-Capely, C. Rouas, M. Benderitter, C. Tessier, Low-concentration uranium enters the HepG2 cell nucleus rapidly and induces cell stress response, Toxicol. In Vitro 30 (2015) 552–560, https://doi.org/10.1016/j.tiv.2015.09.004.
[57] A. Carmona, V. Malard, E. Avazeri, S. Roudeau, F. Porcaro, E. Paredes, C. Vidaud, C. Bresson, R. Ortega, Uranium exposure of human dopaminergic cells results in low cytotoxicity, accumulation within sub-cytoplasmic regions, and down regulation of MAO-B, NeuroToxicology. 68 (2018) 177–188, https://doi.org/10.1016/j.neuro.2018.07.019.
[58] G.J.W. van der Windt, E.L. Pearce, Metabolic switching and fuel choice during T-cell differentiation and memory development, Immunol. Rev. 249 (2012) 27–42, https://doi.org/10.1111/j.1600-065X.2012.01150.x.
[59] Reactome, Image for “Adaptive Immune System”, 2006 (accessed October 18, 2021), https://reactome.org/PathwayBrowser/#/R-HSA-168256.
[60] A.M. Bolt, S. Medina, F.T. Lauer, K.J. Liu, S.W. Burchiel, Minimal uranium immunotoxicity following a 60-day drinking water exposure to uranyl acetate in male and female C57BL/6J mice, Toxicol. Appl. Pharmacol. 372 (2019) 33–39, https://doi.org/10.1016/j.taap.2019.04.003.
[61] M. Goumenou, A. Tsatsakis, Proposing new approaches for the risk characterisation of single chemicals and chemical mixtures: the source related Hazard Quotient (HQS) and Hazard Index (HIS) and the adversity specific Hazard Index (HIA), Toxicol. Rep. 6 (2019) 632–636, https://doi.org/10.1016/j.toxrep.2019.06.010.